nature COMMUNICATIONS

ARTICLE

Received 4 Feb 2013 | Accepted 2 May 2013 | Published 7 Jun 2013

DOI: 10.1038/ncomms2964

Collagen VI regulates satellite cell self-renewal and muscle regeneration

Anna Urciuolo[1], Marco Quarta[2,*], Valeria Morbidoni[1,*], Francesca Gattazzo[1,*], Sibilla Molon[1], Paolo Grumati[1], Francesca Montemurro[3], Francesco Saverio Tedesco[4], Bert Blaauw[1], Giulio Cossu[4], Giovanni Vozzi[3], Thomas A. Rando[2] & Paolo Bonaldo[1]

Adult muscle stem cells, or satellite cells have essential roles in homeostasis and regeneration of skeletal muscles. Satellite cells are located within a niche that includes myofibers and extracellular matrix. The function of specific extracellular matrix molecules in regulating SCs is poorly understood. Here, we show that the extracellular matrix protein collagen VI is a key component of the satellite cell niche. Lack of collagen VI in *Col6a1*$^{-/-}$ mice causes impaired muscle regeneration and reduced satellite cell self-renewal capability after injury. Collagen VI null muscles display significant decrease of stiffness, which is able to compromise the *in vitro* and *in vivo* activity of wild-type satellite cells. When collagen VI is reinstated *in vivo* by grafting wild-type fibroblasts, the biomechanical properties of *Col6a1*$^{-/-}$ muscles are ameliorated and satellite cell defects rescued. Our findings establish a critical role for an extracellular matrix molecule in satellite cell self-renewal and open new venues for therapies of collagen VI-related muscle diseases.

[1] Department of Biomedical Sciences, University of Padova, Padova 35131, Italy. [2] Department of Neurology and Neurological Sciences, Glenn Laboratories for the Biology of Aging, Stanford University School of Medicine, Stanford, California 94305, USA. [3] Interdepartmental Research Center E. Piaggio, University of Pisa, Pisa 56126, Italy. [4] Department of Cell and Developmental Biology, University College London, London WC1E 6DE, UK. * These authors contributed equally to this work. Correspondence and requests for materials should be addressed to P.B. (email: bonaldo@bio.unipd.it) or to T.A.R. (email: rando@stanford.edu).

Interactions between cells and extracellular matrix (ECM) have key roles in tissues undergoing extensive mechanical stress, such as skeletal muscles[1]. A major component of the ECM of skeletal muscles is collagen VI, a protein composed by three genetically distinct chains and forming a discrete network of beaded microfilaments in the basement membrane of muscle endomysium[2,3]. Collagen VI deposition in skeletal muscles is mainly provided by interstitial muscular fibroblasts[4]. Moreover, expression of collagen VI genes is regulated by myogenic cells, whose presence is a prerequisite for inducing the deposition of collagen VI by fibroblasts[5]. The critical role of collagen VI in skeletal muscles is supported by the fact that mutations of *COL6* genes in humans cause various muscle disorders, including Bethlem myopathy and Ullrich congenital muscular dystrophy[2,3]. Collagen VI null (*Col6a1*$^{-/-}$) mice display a mild myopathic phenotype associated with mitochondrial dysfunction, defective autophagy and spontaneous apoptosis of muscle fibers[6–8].

Satellite cells (SCs) are located between the basal lamina and the plasma membrane of muscle fibers[9], and this anatomic localization represents their niche. This niche is characterized by an asymmetric distribution of muscle components, where SCs contact myofibers through the apical surface whereas the ECM lies on their basal surface[9,10]. The myogenic commitment and differentiation of SCs is under the control of key transcription factors, such as the paired box protein 7 (Pax7) and the myogenic regulatory factors MyoD and Myogenin (MyoG)[11–15]. During muscle regeneration, SCs undergo proliferation, generating both a stem cell population by self-renewal and more differentiated cells that give rise to myoblasts that undergo terminal differentiation and fusion[16]. A growing body of evidence indicates that the niche serves as an instructive environment by which SCs respond to extrinsic stimuli associated with muscle growth and repair[17–23]. Changes in the ECM composition provide regulatory cues to SCs, thus influencing their quiescence, activation, differentiation and/or self-renewal[24]. On the other hand, ECM composition affects the mechanical properties of tissue microenvironment, which in turn influence the activity of various stem cells, including SCs[25,26].

Here, we demonstrate that collagen VI is a critical component of SC niche that is required for preserving SC self-renewal and muscle regeneration. *In vitro* and *in vivo* data indicate that one key mechanism through which collagen VI regulates SC activity is the modulation of muscle stiffness. Grafting with wild-type fibroblasts elicits extensive deposition of collagen VI and rescues SC self-renewal and muscle stiffness in *Col6a1*$^{-/-}$ mice. Our findings provide novel insights into the relevance of collagen VI for skeletal muscles and reveal an unforeseen role for this ECM molecule in the regulation of SC homeostasis.

Results

Collagen VI is an extracellular component of SC niche. We first evaluated collagen VI synthesis and localization with respect to SCs in murine extensor digitorum longus (EDL) and tibialis anterior (TA) muscles. Collagen VI was abundant in the endomysium of both muscles, and the protein was adjacent to the surface of SCs (Fig. 1a and Supplementary Fig. S1a). The localization was also confirmed *ex vivo* on freshly isolated myofibers and on sorted SCs (Fig. 1b; Supplementary Fig. S1b,c and Supplementary Movies). Interestingly, collagen VI was expressed by sorted SCs, and *Col6a1* transcripts were regulated during SC activation. Differently from collagen I (the major collagen of muscle interstitial ECM), *Col6a1* transcripts were abundant in quiescent SCs and their amount decreased in activated SCs (Fig. 1c and Supplementary Table S1). When TA muscles were subjected to injury with cardiotoxin[27], collagen VI deposition was markedly increased during the initial phases of regeneration and the protein was found nearby all Pax7^{+} cells 4 days after injury (Fig. 1d,e and Supplementary Figs. S1d and S2). These data indicate that collagen VI is expressed by SCs in a regulated manner and is an ECM component of the niche whose deposition is markedly increased upon muscle regeneration.

Lack of collagen VI affects SCs and muscle regeneration. Based on the above findings, we used collagen VI null (*Col6a1*$^{-/-}$) mice to explore the role of collagen VI in regulating SC function. In addition to abnormalities of muscle fibers in *Col6a1*$^{-/-}$ mice (a higher incidence of centrally nucleated fibers and a lower mean myofiber cross-sectional area), there was an increased number of SCs, with a corresponding increase of SC proliferation and apoptosis, when compared with wild-type muscles (Supplementary Figs. S3 and S4).

We next subjected wild-type and *Col6a1*$^{-/-}$ muscles to cardiotoxin injury. Despite the higher number of SCs before injury, *Col6a1*$^{-/-}$ TA muscles displayed smaller newly forming myofibers 7 days after injury and the number of SCs between *Col6a1*$^{-/-}$ and wild-type TA muscles was markedly reduced when compared with untreated animals (Fig. 2a and Supplementary Fig. S5a). To assess whether the observed alterations were simply due to delayed regeneration in *Col6a1*$^{-/-}$ muscles, we analyzed TA 30 days after injury, when the late myogenic differentiation program was completed. Despite an increase of myofiber cross-sectional area, regenerated *Col6a1*$^{-/-}$ muscles displayed a decreased number of SCs compared with untreated muscles (Fig. 2b and Supplementary Fig. S5b). These results indicate that lack of collagen VI leads to a decreased ability to properly maintain the SC pool after muscle damage, without any overt impairment of the differentiation and fusion of the SC progeny. To ascertain whether this phenotype was caused by a defective self-renewal ability of SCs, we performed multiple injury experiments and analyzed muscles 7 and 30 days after the last injury (Supplementary Fig. S5c). The inability of collagen VI-deficient muscles to regenerate properly after multiple rounds of injury was very evident. Following double injury, *Col6a1*$^{-/-}$ TA muscles displayed a significantly lower number of newly forming myofibers 7 days after injury and a decrease of both myofiber cross-sectional area and muscle mass after 30 days (Fig. 2c,d and Supplementary Fig. S5d,e). This was even more striking in triple injury experiments, where muscle regeneration was dramatically impaired in *Col6a1*$^{-/-}$ TA muscles, with extensive fibrotic lesions and significant decrease of muscle mass, while wild-type TA muscles were still able to regenerate properly (Fig. 2c,d and Supplementary Fig. S5d,f). Notably, following repeated injuries, *Col6a1*$^{-/-}$ TA muscles showed a progressive decline in SC number (Fig. 2e). The progressive depletion of the SC pool in *Col6a1*$^{-/-}$ muscles after injury indicates that collagen VI is strictly needed for the correct function of the niche and the maintenance of SC pool during muscle regeneration.

Collagen VI regulates SC activity *in vitro*. Based on these results, we used different *in vitro* approaches to analyze the effects elicited by collagen VI on SCs. Sorted SCs were prepared from wild-type and *Col6a1*$^{-/-}$ hindlimb muscles and cultured for 48 h on matrigel-coated dishes in the presence or absence of purified native collagen VI. To analyze the differentiation program, we divided cultured SCs into different populations. Early differentiation was evaluated on the basis of Pax7 and MyoD expression, by classifying cells in Pax7^{+}MyoD^{-}, Pax7^{+}MyoD^{+} and Pax7^{-}MyoD^{+} populations[28], whereas the onset of terminal differentiation was evaluated based on MyoG expression and by dividing cells into Pax7^{+}MyoG^{-} and Pax7^{-}MyoG^{+}

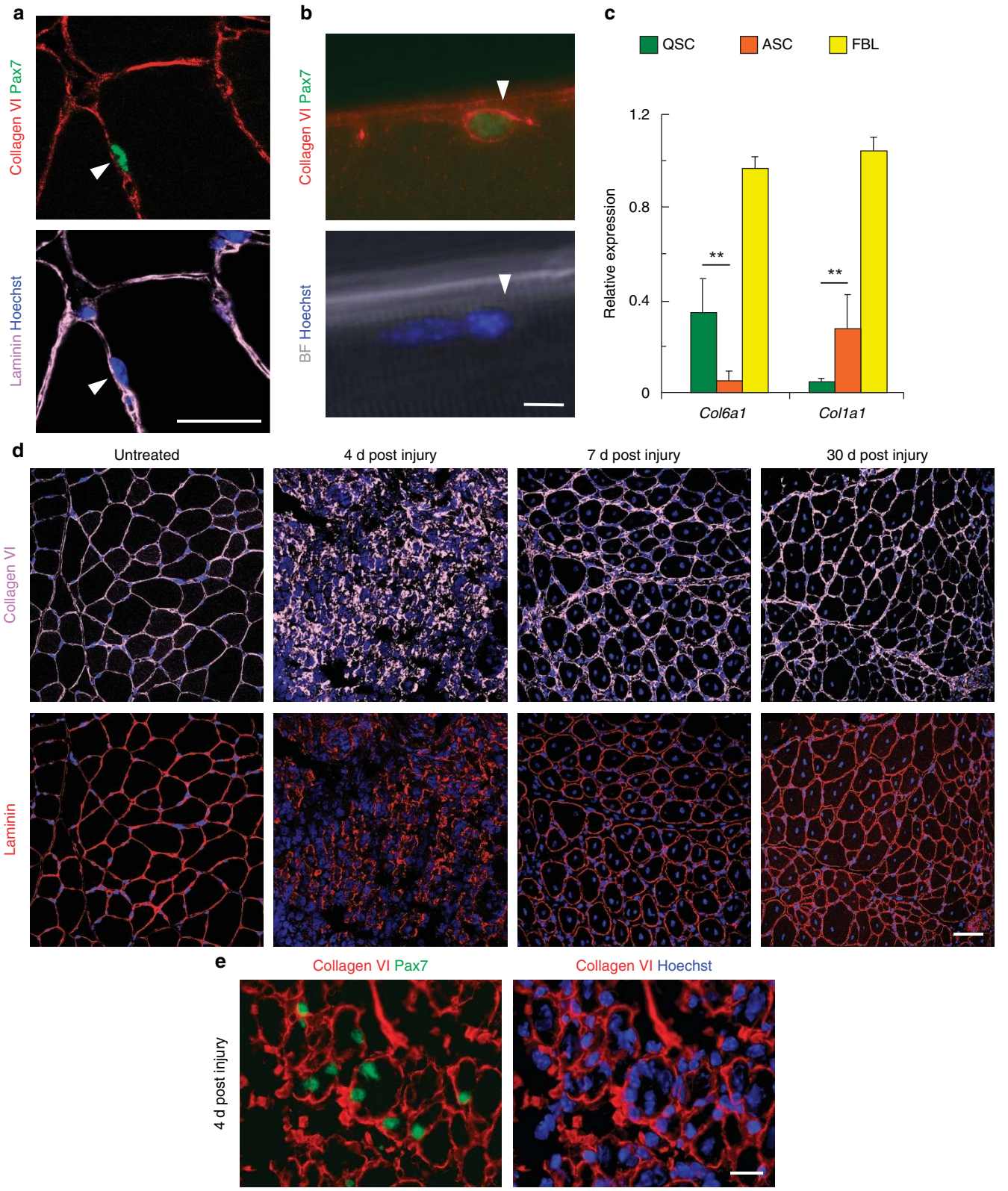

Figure 1 | Collagen VI is an extracellular component of SC niche. (**a**) Representative confocal image of immunofluorescence analysis for collagen VI (red), Pax7 (green) and laminin (light pink) in TA cross-sections from wild-type mice. The arrowhead points at one SC. Scale bar, 25 μm. (**b**) Representative confocal image of a freshly isolated wild-type EDL fiber, showing the immunolocalization of collagen VI (red) with respect to SC (green, arrowhead). BF, bright field. Scale bar, 10 μm. (**c**) Expression levels of *Col6a1* and *Col1a1* transcripts in quiescent (QSC) and activated (ASC) wild-type SCs and in wild-type muscle fibroblasts (FBL). *Gapdh* expression was used to calculate the relative expression of *Col6a1* and *Col1a1* transcripts. Data are shown as mean ± s.e.m. of three independent replicates (**$P<0.01$; unequal variance Student's *t*-test; $n=8$, each group). (**d**) Representative confocal z-stack images of immunofluorescence for collagen VI (light pink) and laminin (red) in TA cross-sections from wild-type mice under untreated conditions or 4 days, 7 days and 30 days after single cardiotoxin injury. Scale bar, 50 μm. (**e**) Representative views of immunofluorescence for collagen VI (red) and Pax7 (green) in wild-type TA 4 days after cardiotoxin injection. Nuclei were stained with Hoechst (blue). Scale bar, 50 μm.

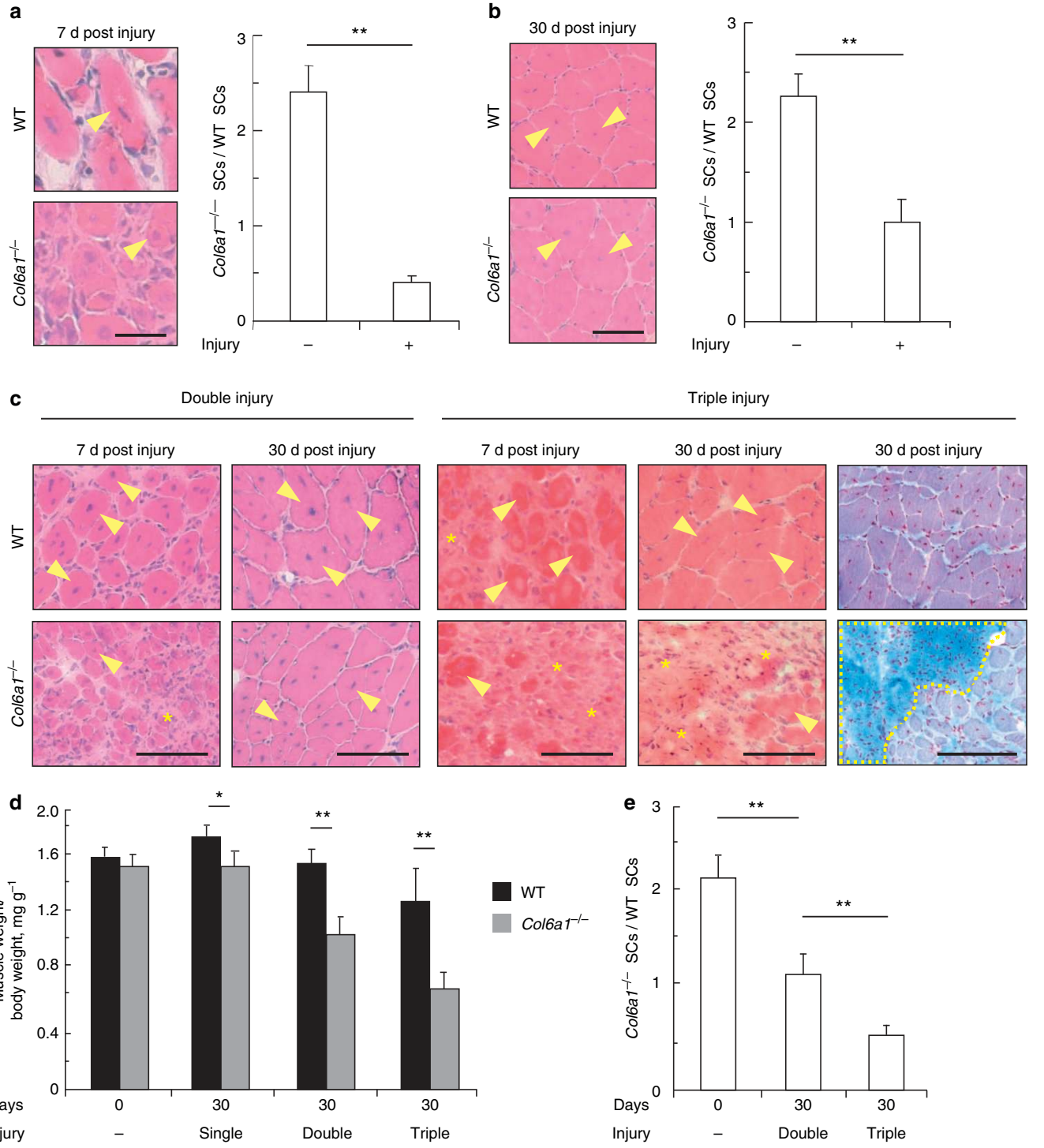

Figure 2 | Lack of collagen VI affects SC maintenance and muscle regeneration *in vivo*. (**a**) Left panel, haematoxylin-eosin staining of TA cross-sections from wild-type and *Col6a1*$^{-/-}$ mice 7 days after cardiotoxin injury. The arrowheads point at some newly forming myofibers. Scale bar, 25 μm. Right panel, ratio of SCs between *Col6a1*$^{-/-}$ and wild-type TA in untreated conditions (−) and 7 days after single injury (+). Data are shown as mean ± s.e.m of three independent replicates (**$P<0.01$; unequal variance Student's *t*-test; $n=6$ animals, each group). (**b**) Left panel, haematoxylin-eosin staining of TA cross-sections from wild-type and *Col6a1*$^{-/-}$ mice 30 days after cardiotoxin injury. The arrowheads point at some newly forming myofibers. Scale bar, 50 μm. Right panel, ratio of SCs between *Col6a1*$^{-/-}$ and wild-type TA in untreated conditions (−) and 30 days after single injury (+). Data are shown as mean ± s.e.m. of three independent replicates (**$P<0.01$; unequal variance Student's *t*-test; $n=6$ animals, each group). (**c**) Haematoxylin-eosin and Azan staining of TA cross-sections from wild-type and *Col6a1*$^{-/-}$ mice 7 days and 30 days after double and triple injury. Arrowheads point at some newly forming myofibers, asterisks label some areas still in the degeneration phase, and the dotted region in the lower right panel show fibrotic tissue substitution stained by Azan. Scale bar, 50 μm. (**d**) Quantification of TA weight/body weight of wild type and *Col6a1*$^{-/-}$ mice in untreated conditions (−) and 30 days after single, double or triple injury. Data are shown as mean ± s.e.m. of three independent replicates (*$P<0.05$; **$P<0.01$; unequal variance Student's *t*-test; $n=6$–8 animals, each group). (**e**) Ratio of SCs between *Col6a1*$^{-/-}$ and wild-type TA in untreated conditions (−) and 30 days after double or triple injury. Data are shown as mean ± s.e.m. of three independent replicates (**$P<0.01$; unequal variance Student's *t*-test; $n=6$ animals, each group). WT, wild-type.

populations[13–15]. When grown on matrigel, *Col6a1*$^{-/-}$ cultures displayed lower percentages of Pax7-expressing cells and corresponding higher percentages of cells expressing MyoD or MyoG. By contrast, growth on collagen VI led to a significant increase of Pax7-expressing cells and decrease of differentiating cells in both wild-type and *Col6a1*$^{-/-}$ cultures (Supplementary Fig. S6a–c and Supplementary Tables S2 and S3).

With the aim to reconstitute the ECM components found in the wild-type SC niche, we analyzed *Col6a1*$^{-/-}$ single fibers cultured for 72 h on matrigel in the absence or presence of collagen VI. *Col6a1*$^{-/-}$ SCs displayed a lower ability to preserve the Pax7^{+}MyoD^{-} population in single fiber culture, as observed in SC-derived culture (Fig. 3a,b and Table 1). When grown on dishes coated with purified collagen VI, *Col6a1*$^{-/-}$ fibers contacted the collagen VI network, which also localized nearby SCs (Fig. 3c and Supplementary Fig. S6d). Remarkably, *Col6a1*$^{-/-}$ SCs showed a higher ability to maintain the Pax7^{+}MyoD^{-} population when fibers were grown on purified collagen VI, with decreased apoptosis and increased proliferation when compared with cultures grown on matrigel alone (Fig. 3a,d,e). Taken together, these *in vitro* data indicate that collagen VI improves the maintenance and survival of cells expressing Pax7, a transcription factor critical for SC self-renewal after damage[11–14].

Collagen VI regulates SC activity *in vivo*. To assess whether the SC defects of collagen VI-deficient muscles may be secondary to the myopathic phenotype, we performed additional *in vivo* studies on *Col6a1*$^{-/-}$ mice. Our previous work established that the myopathic phenotype of *Col6a1*$^{-/-}$ mice is caused by a failure of the autophagic machinery in myofibers, a process that can be reinstated by feeding mice with a low-protein diet or treating them with rapamycin[8]. Based on this, we investigated whether the abnormal activity displayed by SC in *Col6a1*$^{-/-}$ mice is secondary to the myopathic phenotype. Toward this aim, we assessed whether reactivation of autophagy in myofibers, and the consequent rescue of the myopathy, may influence the activity of *Col6a1*$^{-/-}$ SCs. Interestingly, recovery of the autophagy-dependent myofiber defects did not exert any effect on SC activity of *Col6a1*$^{-/-}$ mice, neither in undamaged muscles nor after cardiotoxin injury (Supplementary Fig. S7).

To definitely uncouple the *Col6a1*$^{-/-}$ SC defects from the myopathy, we transplanted wild-type or *Col6a1*$^{-/-}$ SCs into regenerating *Col6a1*$^{-/-}$ muscle and analyzed their function in the host tissue. Indeed, if collagen VI has a direct effect on SCs *in vivo*, the protein expressed by transplanted wild-type cells should enable SCs to function normally in the host tissue and muscle regeneration should be significantly improved. Towards this aim, we sorted GFP^{+} SCs derived from wild-type (WTSCs) and *Col6a1*$^{-/-}$ (KOSCs) mice and injected them into cardiotoxin-injured *Col6a1*$^{-/-}$ muscles (Fig. 4a). Real-time PCR confirmed the presence of donor WTSCs and KOSCs in host muscles and revealed expression of collagen VI in *Col6a1*$^{-/-}$ muscles transplanted with WTSCs (Fig. 4b,c). Notably, the number of SCs in *Col6a1*$^{-/-}$ muscles transplanted with WTSCs was significantly higher than *Col6a1*$^{-/-}$ muscles transplanted with KOSCs (Fig. 4d). Concurrently, muscle regeneration was noticeably improved when *Col6a1*$^{-/-}$ muscles were transplanted with WTSCs, compared with *Col6a1*$^{-/-}$ muscles transplanted with KOSCs (Fig. 4e). These data confirm that the alterations displayed by SCs in *Col6a1*$^{-/-}$ mice are strictly dependent on the lack of collagen VI and indicate that the production of this protein by SCs is required for their proper activity during muscle regeneration.

Collagen VI affects SCs by regulating muscle stiffness. Having established a role for collagen VI in regulating SC activity and muscle regeneration, we investigated the mechanism involved in this process. Although regulation of autophagy is a major mechanism through which collagen VI regulates myofiber homeostasis[8], the results discussed above exclude this mechanism as a determinant for collagen VI regulation of SC activity (Supplementary Fig. S7).

Given the abundance of collagen VI beaded microfilaments in endomysial basement membrane[29], we investigated whether collagen VI may be engaged in the regulation of muscle mechanical properties. Previous work demonstrated that differentiation of stem cells into myoblasts requires optimal tissue elasticity, closely matching the physiological stiffness of skeletal muscle[30]. Moreover, recent studies showed that SCs cultured on bioengineered structures mimicking muscle physiological elasticity display higher *in vitro* self-renewal and *in vivo* regeneration capabilities, when compared with cells grown on plastic[25]. To assess the contribution of collagen VI to muscle mechanical properties, we compared the stiffness of wild-type and *Col6a1*$^{-/-}$ TA muscles using a stress–strain test. Quantification of the Young modulus, an index of elasticity, revealed that *Col6a1*$^{-/-}$ muscles are more elastic ($E \sim 7$ kPa) than their wild-type counterparts ($E \sim 12$ kPa) (Fig. 5a and Supplementary Fig. S8a). *Col6a1*$^{-/-}$ muscles also maintained lower stiffness 4 days after cardiotoxin injury, when there is massive ECM production, indicating that the abnormal elasticity elicited by the lack of collagen VI cannot be compensated by the increased global deposition of other ECM proteins (Fig. 5a and Supplementary Fig. S8a). To investigate whether the observed changes in the mechanical properties of *Col6a1*$^{-/-}$ muscles have any major influence on *in vitro* SC activity, we isolated SCs from wild-type and *Col6a1*$^{-/-}$ GFP^{+} muscles and used them to obtain SC cultures grown on biomimetic structures with a stiffness of either ~7 kPa or ~12 kPa (Supplementary Fig. S8b). Wild-type SCs grown on structures of physiological (12 kPa) stiffness maintained a large proportion of Pax7^{+}MyoD^{-} cells (~70% of total myogenic cells), while this proportion was dramatically decreased (<8% of total myogenic cells) when SCs were grown on structures of 7-kPa stiffness, with a corresponding increase of Pax7^{+}MyoD^{+} and Pax7^{-}MyoD^{+} cells (Fig. 5b). Notably, the total cell numbers for both wild-type and *Col6a1*$^{-/-}$ genotypes were also markedly lower when SCs were cultured on the 7-kPa structures compared with the 12-kPa structures (Supplementary Fig. S8c). Altogether, this set of findings reveals that collagen VI is necessary to maintain muscle mechanical properties *in vivo* and that the altered stiffness displayed by *Col6a1*$^{-/-}$ muscles affects the maintenance of Pax7^{+} cells *in vitro*.

We next assessed the *in vivo* fate of SCs cultured on 7-kPa or 12-kPa biomimetic structures by injecting them into *Col6a1*$^{-/-}$ TA muscles (Fig. 5c). The presence of donor cells in host muscles led to the induction of muscle regeneration as expected, with no significant differences between cells cultured on structures of different stiffness (Fig. 5d,e). Conversely, the number of SCs was significantly increased in muscles transplanted with SCs grown on the 12-kPa structures, but not in those transplanted with SCs grown on the 7-kPa structures (Fig. 5f). Interestingly, several Pax7^{+} cells were found in the interstitium of muscles transplanted with SCs cultured on the less stiff structures (Supplementary Fig. S8d), suggesting that these myogenic cells are less able to adopt a SC localization compared with SCs cultured on structures of physiological stiffness. To get a more precise evaluation of the *in vivo* fate of SCs, we quantified the number of SCs associated with centrally nucleated fibers and found that it was significantly higher in regenerating fibers in muscles transplanted with SCs grown on the 12-kPa structures

(Fig. 5g). Altogether, these data indicate that SCs grown on structures mimicking the stiffness of wild-type muscle have a higher ability to preserve their stem cell function compared with SCs grown on structures mimicking the stiffness of collagen VI-deficient muscles, supporting the idea that matrix stiffness may be a key mechanism through which collagen VI exerts its effects on SCs.

Collagen VI restoration rescues SC self-renewal and muscle stiffness. Previous studies established that fibroblasts are the main producers of collagen VI in skeletal muscles[5]. Based on this, and with the aim to test the effect on SCs and muscle stiffness when collagen VI deposition is reinstated in *Col6a1*$^{-/-}$ mice, we performed grafting experiments with muscle fibroblasts in TA muscles. Fibroblasts were isolated from hindlimb muscles of

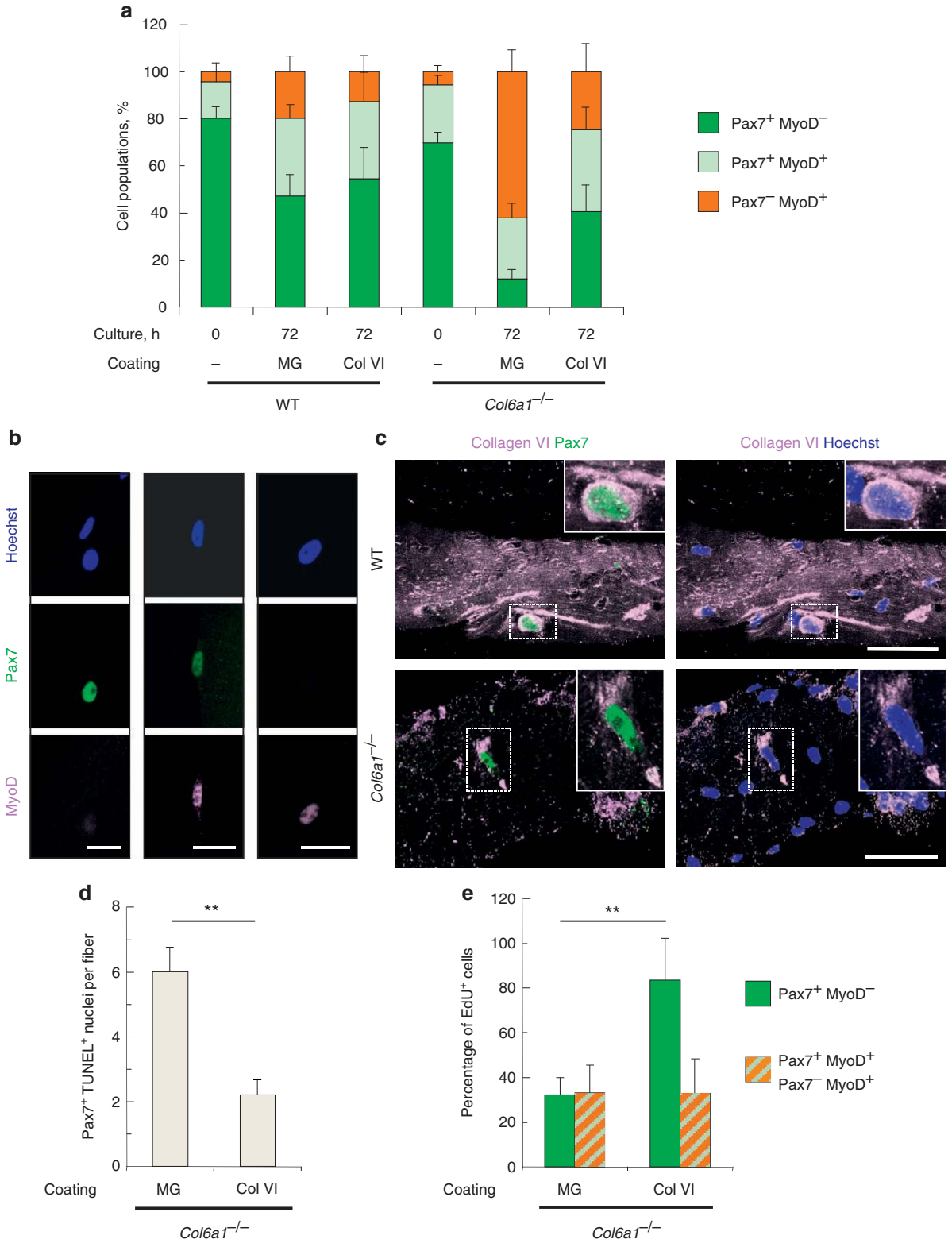

either wild-type (WTFB), GFP transgenic (GFPFB) or *Col6a1*$^{-/-}$ (KOFB) mice, characterized by immunofluorescence (Supplementary Fig. S9a) and injected into TA muscles of *Col6a1*$^{-/-}$ mice. Fibroblasts were found in the connective tissue of *Col6a1*$^{-/-}$ muscles, and WTFBs, but not KOFBs, produced and secreted collagen VI (Fig. 6a and Supplementary Fig. S9b,c). By 4 days after injection, fibroblasts were more diffuse and collagen VI was largely localized in the endomysium nearby Pax7^{+} cells (Fig. 6a,b and Supplementary Fig. S9b,c). To improve collagen VI deposition and overcome the potential loss of fibroblasts by an immune reaction against GFP[31], WTFBs or KOFBs were used and wild-type and *Col6a1*$^{-/-}$ mice were subjected to a second graft 6 days after the initial cell injection. Collagen VI was extensively produced and deposited around myofibers of *Col6a1*$^{-/-}$ muscles subjected to double grafting with WTFBs (Supplementary Fig. S9d).

We next investigated the effects of collagen VI deposition, by comparing wild-type and *Col6a1*$^{-/-}$ TA muscles subjected to injection with either WTFBs or KOFBs. Notably, *Col6a1*$^{-/-}$ TA muscles showed a significant increase of the Young modulus 12 days after grafting with WTFBs, while this physical parameter remained unchanged after grafting with KOFBs (Fig. 6c and Supplementary Fig. S9e). Independently from the genotype of grafted cells, injection of fibroblasts generated a response of SCs in wild-type muscles, as displayed by the local increase of centrally nucleated fibers and by the higher number of SCs (Supplementary Fig. S10a). Differently, the local number of SCs in *Col6a1*$^{-/-}$ TA was increased after grafting with WTFBs, with the concurrent increase of centrally nucleated fibers, but was unaffected by grafting with KOFBs (Fig. 6d and Supplementary Fig. S10b). Of note, we did not observe any rescue of the SC number in areas located nearby the engraftment, but lacking collagen VI deposition, suggesting that the effects on SC activity observed in *Col6a1*$^{-/-}$ muscles were elicited by engrafted WTFBs and collagen VI deposition, with no obvious involvement of additional cell types and/or independent paracrine mechanisms (Supplementary Fig. S10b). To assess whether fibroblast grafting and collagen VI deposition could also improve the maintenance of myogenic cells in *Col6a1*$^{-/-}$ muscles after injury, WTFBs were grafted 4 h after a single cardiotoxin injection and mice were killed 30 days later. Interestingly, collagen VI was still present around *Col6a1*$^{-/-}$ myofibers 30 days after injury (Fig. 6e and Supplementary Fig. S10c) and the SC ratio was significantly higher than that of the controlaterally injured non-grafted muscle, whereas no significant changes were observed in muscle weight and myofiber cross-sectional area (Fig. 6f and Supplementary Fig. S10d,e). Altogether, these data support a role for collagen VI in the regulation of *in vivo* muscle mechanical properties, which in turn can affect SC activity.

Discussion

The correct regulation of stem cell activity is crucial for maintaining tissue homeostasis in physiological and pathological conditions, such as after injury and during wound healing. A number of studies support the notion that the niche, a varied set of cells and extracellular factors nearby stem cells or in contact with them, has key roles in maintaining the quiescence and supporting the self-renewal of stem cells, including SCs. Our findings indicate that collagen VI, an ECM protein forming a distinctive microfibrillar system in several organs, is an essential component of muscle SC niche.

A wealth of observations indicates that the ECM undergoes extensive remodeling in the course of muscle regeneration[24]. Muscle substitution by fibrotic connective tissue is a common feature of several conditions, such as aging and Duchenne muscular dystrophy, pointing at a negative effect for excessive production of fibrillar collagens and interstitial ECM components[32]. Despite this, changes of niche composition are essential for proper SC activity during muscle regeneration[19,24]. We found that collagen VI deposition is markedly increased during the initial phases of muscle regeneration, when the protein forms a thick network enclosing myogenic cells. Previous *in vitro* and *in vivo* studies showed that collagen VI in muscle is produced

Table 1 | Quantification of Pax7^{+}MyoD^{-}, Pax7^{+}MyoD^{+} and Pax7^{-}MyoD^{+} cell populations on single wild type and *Col6a1*$^{-/-}$ myofibers.

	Pax7^{+} (P-value)	*Pax7*$^{+}$*MyoD*$^{+}$ (P-value)	*Pax7*$^{-}$*MyoD*$^{+}$ (P-value)
WT, t0 versus MG	<0.01	<0.05	<0.05
KO, t0 versus MG	<0.01	n.s.	<0.01
t0, WT versus KO	n.s.	n.s.	n.s.
MG, WT versus KO	<0.01	n.s.	<0.01
KO, MG versus Col VI	<0.01	n.s.	<0.01
Col VI, WT versus KO	n.s.	n.s.	n.s.

The table reports the statistical analysis of the data shown in Fig. 3a. Unequal variance Student's *t*-test was used and a *P*-value<0.05 was considered statistically significant (n.s., not significant). Col VI, purified collagen VI; KO, *Col6a1*$^{-/-}$; MG, matrigel; t0, freshly isolated fibers; WT, wild type.

Figure 3 | Collagen VI regulates SC activity *in vitro*. (**a**) Quantification of Pax7^{+}MyoD^{-}, Pax7^{+}MyoD^{+} and Pax7^{-}MyoD^{+} cell populations on single wild-type and *Col6a1*$^{-/-}$ myofibers fixed upon isolation (0 h) or following 72 h culture on matrigel-coated dishes in the presence or absence of purified native collagen VI. Data are shown as mean ± s.e.m. of three independent replicates. The statistical analysis is provided in Table 1 (unequal variance Student's *t*-test; $n=10$–22 myofibers, each group). (**b**) Three representative confocal images of cultured single myofibers and labeled with antibodies for Pax7 (green) and MyoD (light pink). Nuclei were stained with Hoechst (blue). Scale bar, 20 μm. (**c**) Confocal z-stack images of wild-type and *Col6a1*$^{-/-}$ fibers grown on purified collagen VI and analyzed by immunofluorescence for collagen VI (light pink) and Pax7 (green). The insets show higher magnifications of the squared areas. Scale bar, 50 μm. (**d**) Quantification of apoptotic Pax7^{+} cells by TUNEL test in *Col6a1*$^{-/-}$ single myofibers following 72 h culture on matrigel-coated dishes in the presence or absence of purified native collagen VI. Data are shown as mean ± s.e.m. of two independent replicates (**$P<0.01$; unequal variance Student's *t*-test; $n=10$ myofibers, each group). (**e**) Quantification of EdU^{+} cells, calculated as the percentage on Pax7^{+}MyoD^{-}, Pax7^{+}MyoD^{+} and Pax7^{-}MyoD^{+} cell populations, in *Col6a1*$^{-/-}$ single myofibers after 72 h culture on matrigel-coated dishes in the presence or absence of purified native collagen VI. Data are shown as mean ± s.e.m. of three independent replicates (**$P<0.01$; unequal variance Student's *t*-test; $n=10$ myofibers, each group). Col VI, collagen VI; KO, *Col6a1*$^{-/-}$; MG, matrigel; WT, wild-type.

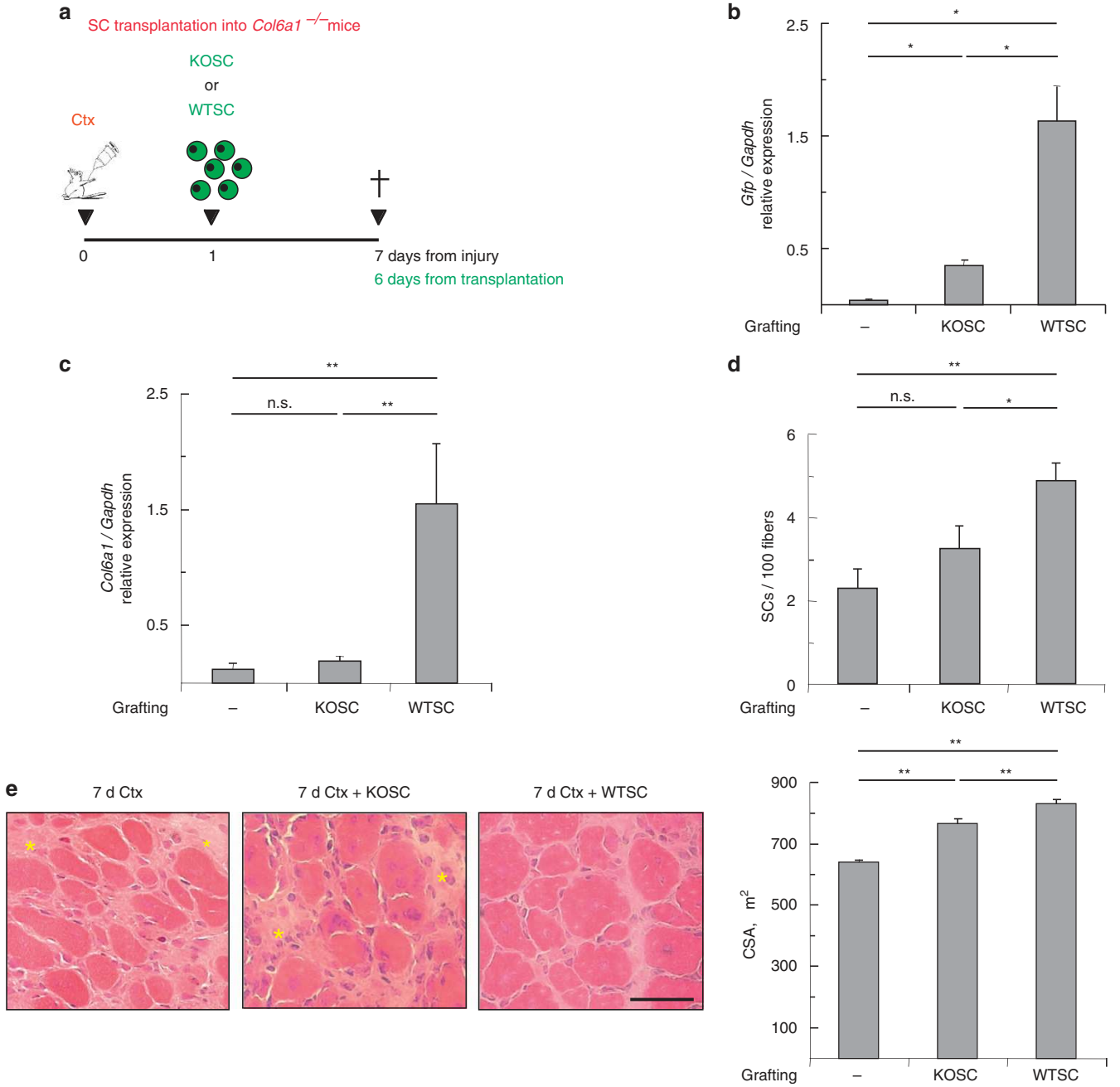

Figure 4 | Collagen VI has a direct effect on SC *in vivo*. (**a**) Schematic diagram of the experimental approach for grafting SCs in *Col6a1*$^{-/-}$ regenerating muscles. One day after cardiotoxin injury, 3,000 freshly isolated wild-type SCs or *Col6a1*$^{-/-}$ SCs expressing the GFP-LC3 fusion protein were injected in regenerating *Col6a1*$^{-/-}$ TA. Muscles were analyzed after 7 days from cardiotoxin injury. (**b**) Real-time PCR analysis of GFP expression in *Col6a1*$^{-/-}$ muscles derived from 7-day cardiotoxin-injured mice without grafting (–) or grafted with wild-type or *Col6a1*$^{-/-}$ SCs expressing GFP-LC3. Data are shown as mean ± s.e.m. of three independent replicates (*$P<0.01$; unequal variance Student's *t*-test; $n=5$ animals, each group). (**c**) Real-time PCR analysis of *Col6a1* expression in *Col6a1*$^{-/-}$ muscles derived from 7-day cardiotoxin-injured mice without grafting (–) or grafted with wild-type SCs or *Col6a1*$^{-/-}$ SCs. Data are shown as mean ± s.e.m. of three independent replicates (**$P<0.01$; n.s., not significant; unequal variance Student's *t*-test; $n=5$ animals, each group). (**d**) Quantification of SCs, calculated as the number of SCs on 100 fibers, in *Col6a1*$^{-/-}$ muscles derived from 7-day cardiotoxin-injured mice without grafting (–) or grafted with 3,000 wild-type SCs or *Col6a1*$^{-/-}$ SCs. Data are shown as mean ± s.e.m. of three independent replicates (**$P<0.01$; * $P<0.05$; n.s., not significant; unequal variance Student's *t*-test; $n=5$–6 animals, each group). (**e**) Left panel, representative images of haematoxylin-eosin staining of TA cross-sections from *Col6a1*$^{-/-}$ mice 7 days after cardiotoxin injury without grafting or grafted with wild-type SCs or *Col6a1*$^{-/-}$ SCs. The asterisks label some areas still in the degeneration phase. Scale bar, 50 μm. Right panel, quantification of myofiber mean cross-sectional area (CSA) in *Col6a1*$^{-/-}$ TA 7 days after cardiotoxin injury without grafting (–) or grafted with wild-type SCs or *Col6a1*$^{-/-}$ SCs. Data are shown as mean ± s.e.m. of three independent replicates (**$P<0.01$; unequal variance Student's *t*-test; $n=5$–6 animals, each group). Ctx, cardiotoxin; KOSC, *Col6a1*$^{-/-}$ SCs expressing GFP-LC3 protein; WTSC, wild-type SCs expressing GFP-LC3.

by endomysial fibroblasts, whereas neither myofibers nor myoblasts produce the protein[4,5]. Here, we found that collagen VI is also expressed by SCs and this expression is differently regulated during quiescence and activation. Our findings suggest that SCs are able to autoregulate the microenvironment of their niche on the basis of their behavior. Indeed, after damage,

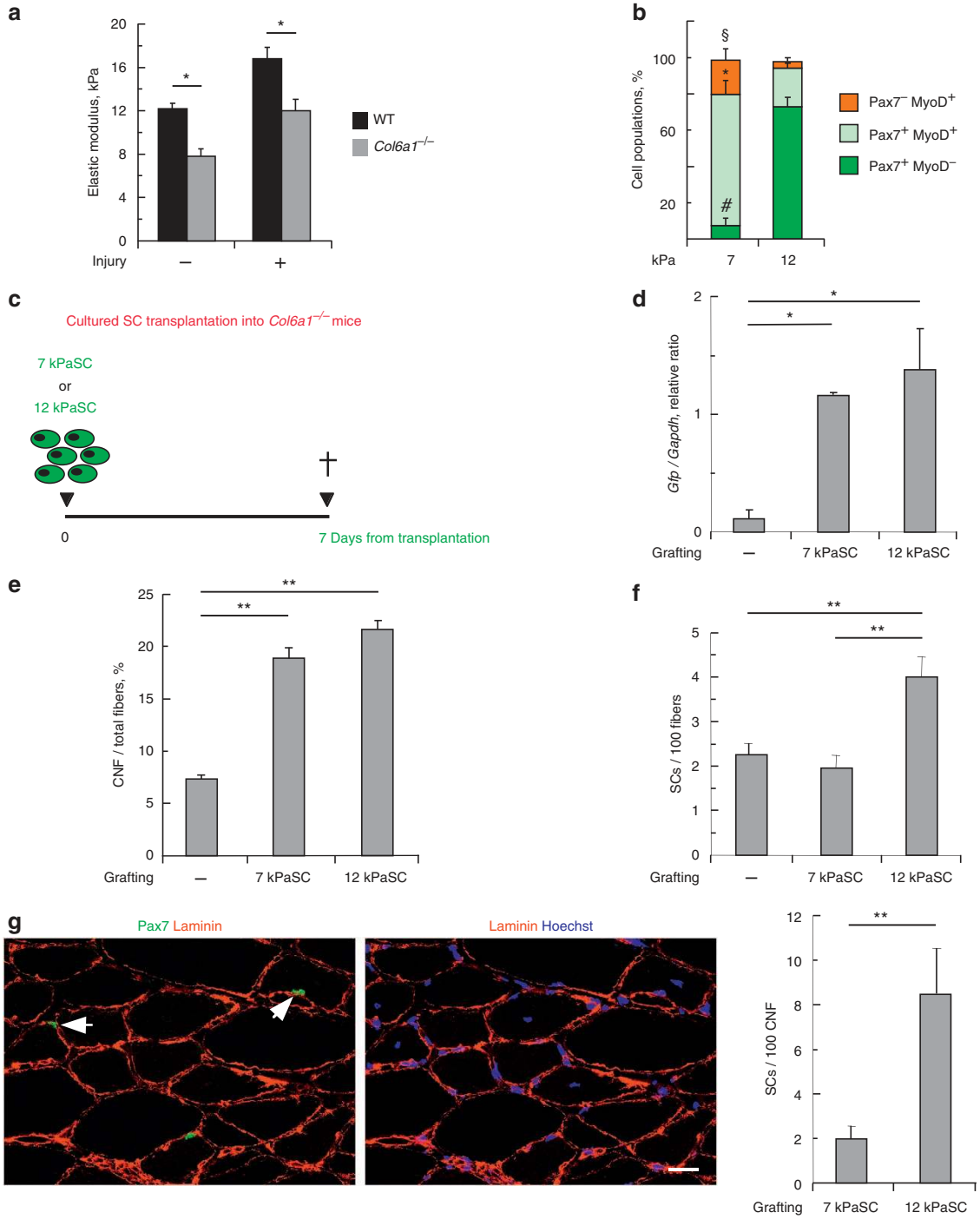

Figure 5 | Collagen VI affects SC self-renewal by regulating muscle stiffness *in vivo*. (**a**) Measurement of elastic modulus of wild-type and *Col6a1*$^{-/-}$ TA muscles under standard conditions (−) and 4 days after injury (+). Data are shown as mean ± s.e.m. of three independent replicates (*$P<0.05$; unequal variance Student's *t*-test; $n=10$ animals, each group). Error bars indicate s.d. (**b**) Quantification of Pax7^{+}MyoD^{-}, Pax7^{+}MyoD^{+}, and Pax7^{-}MyoD^{+} cell populations in sorted wild-type SCs, following 7 days culture on biomimetic structures. Data are shown as mean ± s.e.m of two independent replicates ($^{\#}P<0.01$ for the Pax7^{+}MyoD^{-} population; *$P<0.01$ for the Pax7^{+}MyoD^{+} population; $^{\S}P<0.01$ for the Pax7^{-}MyoD^{+} population; unequal variance Student's *t*-test; $n=8$ wells, each group). (**c**) Schematic diagram of the experimental approach for grafting cultured SCs grown on 7 kPa or 12 kPa in *Col6a1*$^{-/-}$ TA muscles. (**d**) Real-time PCR analysis of GFP DNA content in *Col6a1*$^{-/-}$ TA under untreated condition (−) or after grafting. Data are shown as mean ± s.e.m of three independent replicates (*$P<0.05$; unequal variance Student's *t*-test; $n=6$ animals, each group). (**e**) Analysis of centrally nucleated fibers (CNF) in *Col6a1*$^{-/-}$ TA under untreated condition (−) or 7 days after grafting. Data are shown as mean ± s.e.m. of three independent replicates (**$P<0.01$; unequal variance Student's *t*-test; $n=6$ animals, each group). (**f**) Quantification of SCs in *Col6a1*$^{-/-}$ TA under untreated condition (−) or 7 days after grafting. Data are shown as mean ± s.e.m. of three independent replicates (**$P<0.01$; unequal variance Student's *t*-test; $n=6$ animals, each group). (**g**) Left panel, representative images of *Col6a1*$^{-/-}$ TA grafted with cultured SCs, showing SCs localized in centrally nucleated fibers (CNFs, arrows). Scale bar, 25 μm. Right panel, quantification of SCs in CNFs of *Col6a1*$^{-/-}$ TA under untreated condition (−) or 7 days after grafting. Data are shown as mean ± s.e.m. of three independent replicates (**$P<0.01$; unequal variance Student's *t*-test; $n=6$ animals, each group). 7 kPaSC, wild-type SCs cultured on 7 kPa; 12 kPaSC, wild-type SCs cultured on 12 kPa; Col VI, collagen VI; MG, matrigel; WT, wild-type.

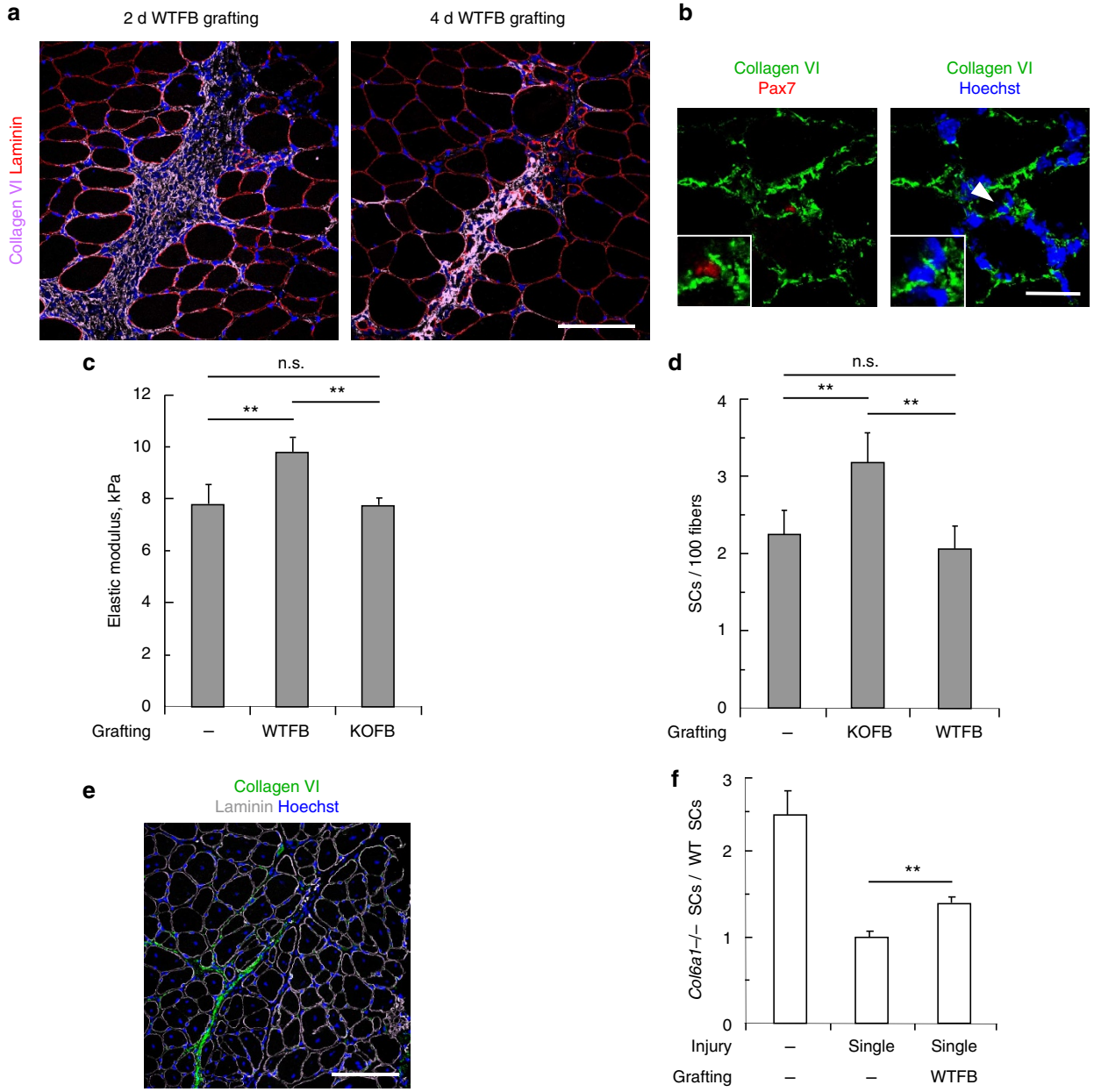

Figure 6 | Wild-type fibroblast grafting rescues SC self-renewal and muscle stiffness in *Col6a1*$^{-/-}$ muscles. (**a**) Representative confocal z-stack image of immunofluorescence analysis of *Col6a1*$^{-/-}$ TA muscles 2 and 4 days after transplantation with wild-type fibroblasts. Sections were labeled with antibodies against collagen VI (light pink) and laminin (red). Scale bar, 100 μm. (**b**) Representative confocal z-stack images of immunofluorescence for collagen VI (green) and Pax7 (red) in *Col6a1*$^{-/-}$ TA sections 4 days after grafting with wild-type fibroblasts. The arrowhead points at one Pax7^{+} cell, shown at higher magnification in the inset. Scale bar, 25 μm. (**c**) Quantification of the elastic modulus of *Col6a1*$^{-/-}$ TA under untreated conditions (–) and 12 days after grafting with wild-type fibroblasts or *Col6a1*$^{-/-}$ fibroblasts. Data are shown as mean ± s.d. of two independent replicates (**$P<0.01$; n.s., not significant; unequal variance Student's *t*-test; $n=10$ animals, each group). (**d**) Quantification of SCs in *Col6a1*$^{-/-}$ TA in untreated conditions (–) and in the graft region 12 days after grafting with wild-type fibroblasts or *Col6a1*$^{-/-}$ fibroblasts. Data are shown as mean ± s.e.m. of three independent replicates (**$P<0.01$; unequal variance Student's *t*-test; n.s., not significant; $n=6$ animals, each group). (**e**) Representative confocal z-stack image of immunofluorescence for collagen VI (green) and laminin (gray) in *Col6a1*$^{-/-}$ TA cross-sections 30 days after injury and grafting with wild-type fibroblasts. Scale bar, 100 μm. (**f**) Ratio of SCs between *Col6a1*$^{-/-}$ and wild-type mice under untreated conditions (–) or 30 days after cardiotoxin injury either in the absence or in the presence of a single grafting with wild-type fibroblasts. Data are shown as mean ± s.e.m. of three independent replicates (**$P<0.01$; unequal variance Student's *t*-test; $n=6$ animals, each group). Nuclei were stained with Hoechst (blue). KOFB, *Col6a1*$^{-/-}$ fibroblasts; WTFB, wild-type fibroblasts.

activated SCs leave their original niche for seeding in a 'new niche' enriched in ECM components, including collagen VI, which are mainly provided by interstitial fibroblasts. In this context, it is plausible that SCs need to change their intrinsic expression of ECM proteins, reducing the synthesis of collagen VI. Interestingly, recent literature studies support this concept by showing that SCs contribute to their own environment through the synthesis of ECM components such as collagens[33,34].

Moreover, it also became evident that the niche not only provides a number of molecular signals for SCs[17–23], but also

establishes a three-dimensional support with specific mechanical properties[10]. Healthy skeletal muscle tissue displays a definite elastic modulus ($E \sim 12$ kPa). These biomechanical properties of muscles are altered during disease, aging and injury, as demonstrated by the stiffer elastic modulus ($E > 18$ kPa) of muscles of dystrophin-deficient *mdx* mice and of aged mice, where SC activity is compromised[10]. Our findings indicate that (i) *Col6a1*$^{-/-}$ muscles display a distinct increase of elasticity, and that (ii) this lower stiffness is associated with a significant loss of *in vitro* and *in vivo* self-renewal capability of wild-type SCs, pointing to altered stiffness as one key mechanism underlying *in vivo* SC defects in collagen VI-deficient muscles.

Independent evidence points to collagen VI as an ECM molecule involved in the regulation of the mechanical properties of the cell microenvironment. For instance, the pericellular matrix of articular cartilage of *Col6a1*$^{-/-}$ mice was found to have a significantly reduced stiffness[35], suggesting a more general biomechanical role for collagen VI in different tissues. Moreover, collagen VI null mice were shown to be resistant to genetically induced mammary tumorigenesis[36], a process known to be particularly sensitive to the mechanical properties of the microenvironment[37,38]. Our findings support the concept of a strict relationship between SC homeostasis and regulation of muscle biomechanical properties (Supplementary Fig. 11)[10,25]. Future studies, aimed at dissecting the molecular factors involved in the transduction of the mechanical signals generated by collagen VI microfilaments in muscle endomysium, will allow a more thorough understanding of the pathways through which collagen VI exerts its effects within the SC niche. Moreover, we cannot exclude possible biochemical benefits of collagen VI on SCs that might also contribute to the observed changes. Actually, such biochemical benefits are also suggested by the *in vitro* effects exerted by collagen VI on wild-type SCs. This scenario, together with the results obtained by transplantation experiments with different cells (freshly isolated SCs, cultured SCs and fibroblasts), suggests that collagen VI is not only important in the regulation of muscle mechanical properties, but may also provide biochemical signals to SCs. Although further studies are needed in this direction, it is intriguing to hypothesize that collagen VI could have a dual function: on one hand it is critical for the regulation of the mechanical properties of skeletal muscle, and on the other hand it may interact with some SC receptors, including those that can modulate the physical perception of the microenvironment surrounding the cells.

Our study also provides new perspectives for human collagen VI diseases, as they represent non-cell-autonomous disorders of muscle[2]. The finding that cultured fibroblasts are able to secrete and deposit collagen VI in host *Col6a1*$^{-/-}$ muscle, with beneficial effects on SCs and muscle stiffness, opens novel therapeutic venues for collagen VI-related muscular dystrophies. In various tissues, fibroblasts represent a source for collagen VI, and dermal fibroblasts derived from skin biopsies have been largely used as a diagnostic tool in patients with collagen VI mutations[3]. The possibility that fibroblasts obtained from minimally invasive biopsies may be grown in culture and used for the production and deposition of collagen VI in muscle *in vivo* is an attractive therapeutic option that remains to be explored in the future.

Methods

Mice. We performed experiments in wild-type mice of the inbred C57BL/6J strain and in *Col6a1*$^{-/-}$ mice that we previously backcrossed in the C57BL/6J strain for eight generations[7]. We obtained data in 6-month-old mice by comparing sex-matched wild-type and *Col6a1*$^{-/-}$ animals. We used C57BL/6J, C57BL/6-Tg(ACTB-EGFP)1Osb/J (Jackson Laboratories) and *Col6a1*$^{-/-}$ mice to isolate muscle fibroblasts for grafting experiments. We used *Col6a1*$^{+/+}$;GFP-LC3 and *Col6a1*$^{-/-}$;GFP-LC3 mice (generated in our laboratory by crossing *Col6a1*$^{-/-}$ mice with GFP-LC3 mice[39]) to isolate SCs for transplantation experiments. Mice were housed in individual cages in an environmentally controlled room (23 °C, 12 h light/12 h dark cycle) and provided food and water *ad libitum*. Native collagen VI was purified from newborn mice as previously described[7]. Mouse procedures were approved by the Ethics Committee of the University of Padova and authorized by the Italian Ministry of Health.

***In vivo* treatments.** For cardiotoxin injury[27], we anesthetized mice with isoflurane (Merial) and injected TA muscles with 30 µl cardiotoxin (*Naja mossambica mossambica*, 10 µM; Sigma). Analgesia (Rimadyl) was administered for 3 days. For multiple injury experiments, TA muscles were injected with cardiotoxin 1 month after the previous injection (see also Supplementary Fig. S4C). For cell proliferation analysis, EdU (Invitrogen) was administered for 7 days by i.p. injection at 50 mg per kg body weight every 12 h. We carried out induction of autophagy by i.p. injection with rapamycin (2 mg per kg body weight; LC Laboratories) every 24 hr for 15 days or by feeding mice with LPD (TestDiet) for 1 month[8]. For SC transplantation, we resuspended 3,000 sorted SCs in 15 µl phosphate buffered saline (PBS) and injected them into TA muscle 24 h after cardiotoxin injury. For transplantation of cultured SCs, sorted SCs were grown in culture for 1 week on biomimetic structures, then 10^4 cells were resuspended in 15 µl PBS and injected into undamaged TA muscle. For grafting with muscle fibroblasts, we resuspended 10^5 cells in 15 µl PBS and injected them into each TA muscle. For double-grafting experiments, we used the same primary culture preparation for both injections and performed the second injection 6 days after the first one.

Isolation and culture of single EDL muscle fibers. We carefully dissected EDL muscles from 6-month-old mice and subjected them to enzymatic digestion with collagenase I (2 mg ml^{-1}, Gibco) for 80 min at 37 °C. We blocked the digestion with Dulbecco's Modified Eagle Medium (DMEM, Sigma) supplemented with 0.2 M L-glutamine (Invitrogen), 1:100 penicillin–streptomycin (Invitrogen), 1:100 fungizone (Invitrogen) and 10% horse serum (Gibco), and gently released single myofibers from muscles. With the aim to remove debris and interstitial cells, every 15–25 min, undamaged and non-contracted fibers were transferred in a new dish containing fresh medium for five times. Single selected fibers were maintained at 37 °C in a cell incubator between each wash cycle. Freshly isolated fibers were finally fixed in 4% paraformaldehyde in PBS for 15 min and maintained at 4 °C in PBS until use. For culture experiments, selected fibers were individually grown in adhesion, by placing them into chamber slides coated for at least 2 h with matrigel alone (ECM gel, Sigma) or with matrigel supplemented with purified collagen VI (5 µg cm^{-2}). We cultured fibers for 72 h at 37 °C in cell incubator, using DMEM supplemented with 20% horse serum, 10% fetal bovine serum (Gibco), 1% chicken embryo extract (Sera Laboratories International) and, where indicated, 10 nM EdU (Invitrogen).

Isolation and culture of SCs. We dissected hindlimb muscles from mice and gently dissociated them with a MACS dissociator (Miltenyi Biotec) to yield fragmented muscle suspensions. We digested muscle suspensions for 90 min in 37 °C shaking water bath, using collagenase II (500 U ml^{-1}, Invitrogen) solution in Ham's F10 medium (Sigma) supplemented with 10% horse serum (Invitrogen). We washed the fragmented myofibers and further digested them for 30 min in 37 °C shaking water bath with collagenase II (100 U ml^{-1}, Invitrogen) and dispase (2 U ml^{-1}, Invitrogen). We triturated the digested cell/fragmented fiber suspensions and washed them to yield mononucleated cell suspensions. We filtered the dissociated suspensions through 70- and 30-µm filters and labeled mononucleated cells with VCAM-biotin (1:100, 429), CD31-APC (1:100, MEC 13.3), CD45-APC (1:100, 30-F11) (all BD Bioscience) and Sca-1-Pacific-Blue (1:100, D7, Biolegend). We used streptavidin-PE-cy7 (1:100, BD Biosciences) to amplify the VCAM signal. Where indicated, single-cell preparations were labeled with anti-mouse CD31 FITC (1:100, 11-0311), anti-mouse CD45 FITC (1:100, 11-0451), anti-mouse Sca-1 FITC (1:100, 11-5981) (all eBioscence) and biotin-anti-SM/C-2.6 (1:100, a gift from S. Fukada[40]). We used streptavidin-PerCP-Cy5.5 (1:100, BD Biosciences) to amplify the SM/C-2.6 signal. We carefully optimized cell sorting for purity and viability and subjected SM/C-2.6$^+$CD45$^-$CD31$^-$Sca1$^-$ or VCAM$^+$CD31$^-$CD45$^-$Sca-1$^-$ cells to FACS analysis right after sorting to ensure SC purity. For culture experiments, 10^4 sorted SCs were plated on dishes coated with matrigel alone (ECM gel, Sigma) or with matrigel supplemented with purified collagen VI (5 µg cm^{-2}), or on biomimetic structures coated with matrigel alone (ECM gel, Sigma). We cultured sorted SCs for 48 h or 7 days at 37 °C in cell incubator, using DMEM supplemented with 20% horse serum, 10% fetal bovine serum (Gibco), 1% chicken embryo extract (Sera Laboratories International) and, where indicated, 10 nM EdU (Invitrogen).

Isolation and culture of muscle fibroblasts. We used hindlimb muscles for preparing primary muscle fibroblasts by enzymatic digestion with collagenase II (100 U ml^{-1}, Invitrogen) and dispase (2 U ml^{-1}, Invitrogen) for 30 min at 37 °C. We filtered the dissociated suspensions through 70- and 30-µm filters and plated them for 10 min on gelatin-coated dishes. After removal of floating cells, we maintained the attached cells in culture until confluence. In order to enrich for fibroblasts, we expanded primary cultures for one further passage until confluence, and prepared them for cell type characterization and grafting.

***In vivo* muscle stiffness.** We carefully dissected TA muscles from mice and subjected them to stress–strain tests with a Zwick/Roell Z005 device (Zwick, Germany). We anchored muscles to the jaws of the device using a suture thread, and subjected them to two consecutive compressive load–unload cycles with the following settings: 0.01 mm s^{-1}, strain rate; 10% strain, end of loading phase (compared with the initial sample length); no load, end of load–unload cycle. We calculated the elastic modulus from the first linear portion of the stress–strain curve for each cycle.

Biomimetic structures. For the generation of biomimetic structures, we prepared a solution of 3% (*w*/*v*) gelatin (Sigma) in PBS or of 5% (*w*/*v*) gelatin in PBS. Genipin (Challenge Bioproducts Co., Ltd) was added to the solutions at 0.2% (*w*/*w*). Each mixture was kept at 40 °C under moderate stirring, until polymerization was completed as indicated by turning into blue color. Samples were left drying at room temperature for 48 h, rinsed in water to remove genipin residues, sterilized under UV light and then kept in PBS until use at 4 °C. The mechanical properties of genipin-crosslinked biomimetic structures were measured with a Zwick/Roell Z005 device. Samples were subjected to compressive load–unload cycles with the following settings parameters: 0.01 mm s^{-1}, strain rate; 10% strain, end of loading phase; no load, end of load–unload cycle. The Young's modulus of each sample was evaluated from the slope of the initial linear portion of the stress–strain curve. Biomimetic structures composed by 3% gelatin were characterized by an elastic modulus of ~7 kPa, whereas those composed by 5% gelatin displayed an elastic modulus of ~12 kPa. At least three specimens for each composition were tested. Biomimetic structures were maintained in culture medium at 37 °C overnight, before SC plating.

Statistical analyses. We expressed data as means ± s.e.m. or, where indicated, as means ± s.d. We determined statistical significance by unequal variance Student's *t*-test. A P-value < 0.05 was considered statistically significant.

Other methods. Additional information on methods is provided in Supplementary Methods.

References

1. Gillies, A. R. & Lieber, R. L. Structure and function of the skeletal muscle extracellular matrix. *Muscle Nerve* **44,** 318–331 (2011).
2. Bönnemann, C. G. The collagen VI-related myopathies: muscle meets its matrix. *Nat. Rev. Neurol.* **21,** 379–390 (2011).
3. Lampe, A. K. & Bushby, K. M. Collagen VI related muscle disorders. *J. Med. Genet.* **42,** 673–685 (2005).
4. Zou, Y., Zhang, R. Z., Sabatelli, P., Chu, M. L. & Bönnemann, C. G. Muscle interstitial fibroblasts are the main source of collagen VI synthesis in skeletal muscle: implications for congenital muscular dystrophy types Ullrich and Bethlem. *J. Neuropathol. Exp. Neurol.* **67,** 144–154 (2008).
5. Braghetta, P. *et al.* An enhancer required for transcription of the Col6a1 gene in muscle connective tissue is induced by signals released from muscle cells. *Exp. Cell Res.* **314,** 3508–3518 (2008).
6. Bonaldo, P. *et al.* Collagen VI deficiency induces early onset myopathy in the mouse: an animal model for Bethlem myopathy. *Hum. Mol. Genet.* **7,** 2135–2140 (1998).
7. Irwin, W. A. *et al.* Mitochondrial dysfunction and apoptosis in myopathic mice with collagen VI deficiency. *Nat. Genet.* **35,** 367–371 (2003).
8. Grumati, P. *et al.* Autophagy is defective in collagen VI muscular dystrophies, and its reactivation rescues myofiber degeneration. *Nat. Med.* **16,** 1313–1320 (2010).
9. Mauro, A. Satellite cell of skeletal muscle fibers. *J. Biophys. Biochem. Cytol.* **9,** 493–495 (1961).
10. Cosgrove, B. D., Sacco, A., Gilbert, P. M. & Blau, H. M. A home away from home: challenges and opportunities in engineering in vitro muscle satellite cell niches. *Differentiation* **78,** 185–194 (2009).
11. Lepper, C., Partrigde, T. A. & Fan, C. M. An absolute requirement for Pax7-positive satellite cells in acute injury skeletal muscle regeneration. *Development* **138,** 3639–3646 (2011).
12. Sambasivan, R. *et al.* Pax7-expressing satellite cells are indispensable for adult skeletal muscle regeneration. *Development* **138,** 3647–3656 (2011).
13. Zammit, P. S., Partridge, T. A. & Yablonka-Reuveni, Z. The skeletal muscle satellite cell: the stem cell that came in from the cold. *J. Histochem. Cytochem.* **54,** 1177–1191 (2006).
14. Yablonka-Reuveni, Z., Day, K., Vine, A. & Shefer, G. Defining the transcriptional signature of skeletal muscle stem cells. *J. Anim. Sci.* **86,** E207–E216 (2008).
15. Ono, Y. *et al.* BMP signalling permits population expansion by preventing premature myogenic differentiation in muscle satellite cells. *Cell Death Differ.* **18,** 222–234 (2011).
16. Tedesco, F. S., Dellavalle, A., Diaz-Manera, J., Messina, G. & Cossu, G. Repairing skeletal muscle: regenerative potential of skeletal muscle stem cells. *J. Clin. Invest.* **120,** 11–19 (2010).
17. Brack, A. S., Conboy, I. M., Conboy, M. J., Shen, J. & Rando, T. A. A temporal switch from Notch to Wnt signaling in muscle stem cells is necessary for normal adult myogenesis. *Cell Stem Cell* **2,** 50–59 (2008).
18. Cornelison, D. D. *et al.* Essential and separable roles for Syndecan-3 and Syndecan-4 in skeletal muscle development and regeneration. *Genes Dev.* **18,** 2231–2236 (2004).
19. Kuang, S., Gillespie, M. A. & Rudnicki, M. A. Niche regulation of muscle satellite cell self-renewal and differentiation. *Cell Stem Cell* **2,** 22–31 (2008).
20. Le Grand, F., Jones, A. E., Seale, V., Scime, A. & Rudnicki, M. A. Wnt7a activates the planar cell polarity pathway to drive the symmetric expansion of satellite stem cells. *Cell Stem Cell* **4,** 535–547 (2009).
21. Pisconti, A., Cornelison, D. D., Olguín, H. C., Antwine, T. L. & Olwin, B. B. Syndecan-3 and Notch cooperate in regulating adult myogenesis. *J. Cell Biol.* **190,** 427–441 (2010).
22. Shea, K. L. *et al.* Sprouty1 regulates reversible quiescence of a self-renewing adult muscle stem cell pool during regeneration. *Cell Stem Cell* **6,** 117–129 (2010).
23. Conboy, I. M. & Rando, T. A. The regulation of Notch signaling controls satellite cell activation and cell fate determination in postnatal myogenesis. *Dev. Cell* **3,** 397–409 (2002).
24. Calve, S., Odelberg, S. J. & Simon, H. G. A transitional extracellular matrix instructs cell behavior during muscle regeneration. *Dev. Biol.* **344,** 259–271 (2010).
25. Gilbert, P. M. *et al.* Substrate elasticity regulates skeletal muscle stem cell self-renewal in culture. *Science* **329,** 1078–1081 (2010).
26. Guilak, F. *et al.* Control of stem cell fate by physical interactions with the extracellular matrix. *Cell Stem Cell* **5,** 17–26 (2009).
27. Couteaux, R., Mira, J. C. & d'Albis, A. Regeneration of muscles after cardiotoxin injury. I. Cytological aspects. *Biol. Cell* **62,** 171–182 (1988).
28. Zammit, P. S. *et al.* Muscle satellite cells adopt divergent fates: a mechanism for self-renewal? *J. Cell Biol.* **166,** 347–357 (2004).
29. Kuo, H. J., Maslen, C. L., Keene, D. R. & Glanville, R. W. Type VI collagen anchors endothelial basement membranes by interacting with type IV collagen. *J. Biol. Chem.* **272,** 26522–26529 (1997).
30. Engler, A. J., Sen, S., Sweeney, H. L. & Discher, D. E. Matrix elasticity directs stem cell lineage specification. *Cell.* **126,** 677–689 (2006).
31. Andersson, G. *et al.* Engraftment of retroviral EGFP-transduced bone marrow in mice prevents rejection of EGFP-transgenic skin grafts. *Mol. Ther.* **8,** 385–391 (2003).
32. Mann, C. J. *et al.* Aberrant repair and fibrosis development in skeletal muscle. *Skelet. Muscle* **1,** 21 (2011).
33. Bentzinger, C. F. *et al.* Fibronectin regulates wnt7a signaling and satellite cell expansion. *Cell Stem Cell* **12,** 75–87 (2013).
34. Bröhl, D. *et al.* Colonization of the satellite cell niche by skeletal muscle progenitor cells depends on Notch signals. *Dev. Cell* **23,** 469–481 (2012).
35. Alexopoulos, L. G., Youn, I., Bonaldo, P. & Guilak, F. Development of osteoarthritic changes in Col6a1-knocnout mice: biomechanics of type VI collagen in cartilage pericellular matrix. *Arthritis Rheum.* **60,** 771–779 (2009).
36. Iyengar, P. *et al.* Adipocyte-derived collagen VI affects early mammary tumor progression *in vivo*, demonstrating a critical interaction in the tumor/stroma microenvironment. *J. Clin. Invest.* **115,** 1163–1176 (2005).
37. Levental, K. R. *et al.* Matrix crosslinking forces tumor progression by enhancing integrin signaling. *Cell* **139,** 891–906 (2009).
38. Lopez, J. I., Kang, I., You, W. K., McDonald, D. M. & Weaver, V. M. In situ force mapping of mammary gland transformation. *Integr. Biol. (Camb.)* **3,** 910–921 (2011).
39. Mizushima, N., Yamamoto, A., Matsui, M., Yoshimori, T. & Ohsumi, Y. *In vivo* analysis of autophagy in response to nutrient starvation using transgenic mice expressing a fluorescent autophagosome marker. *Mol. Biol. Cell* **15,** 1101–1111 (2004).
40. Fukada, S. *et al.* Purification and cell-surface marker characterization of quiescent satellite cells from murine skeletal muscle by a novel monoclonal antibody. *Exp. Cell Res.* **296,** 245–255 (2004).

Acknowledgements

We thank S. Dupont and M. Montagner for helpful discussion, L. Vitiello and A. Cabrelle for advices and technical help, and S. Piccolo for critical reading of the manuscript. We are grateful to N. Mizushima for the GFP-LC3 mice, S. Fukada for the SM/C-2.6 antibody and R. Wagener for the α3(VI) antibody. This work was financially supported by Telethon-Italy Grants GGP10225 and GGP11082, Italian Ministry of Education, University and Research Grant RBAP11Z3YA_003, and University of Padova Strategic Projects (to P.B.); Glenn Foundation for Medical Research, NIH Grants P01 AG036695, R01 AR56849, DP1 OD000392 (an NIH Director's Pioneer Award), Department of Veterans Affairs (Merit Review) (to T.A.R.).

Author contributions

A.U. planned and performed most *in vivo* and *in vitro* experiments and wrote the paper. M.Q. carried out the analysis of collagen VI production by SCs. V.M. performed *in vivo* SC quantification. F.G. generated and characterized biomimetic structures and performed myofiber studies. S.M. performed histological analysis and myofiber studies. P.G. and B.B. performed mouse genotyping and treatments. F.M. and G.V. provided the mechanical analysis. F.S.T. was involved in muscle injury experiments. G.C. provided conceptual advice and was involved in data analysis. T.A.R. oversaw the results and was involved in data analysis. P.B. coordinated the study, oversaw the results and wrote the paper. All authors discussed the results and commented on the manuscript.

Additional information

Supplementary Information accompanies this paper at http://www.nature.com/naturecommunications

Competing financial interests: The authors declare no competing financial interests.

Reprints and permission information is available online at http://npg.nature.com/reprintsandpermissions/

How to cite this article: Urciuolo, A. *et al.* Collagen VI regulates satellite cell self-renewal and muscle regeneration. *Nat. Commun.* 4:1964 doi: 10.1038/ncomms2964 (2013).